Science of the Total Environment 803 (2022) 149738

Contents lists available at ScienceDirect

Science of the Total Environment

journal homepage: www.elsevier.com/locate/scitotenv

Field comparison of passive polyurethane foam and active air sampling techniques for analysis of gas-phase semi-volatile organic compounds at a remote high-mountain site

Raimon M. Prats *, Barend L. van Drooge, Pilar Fernández, Joan O. Grimalt

Institute of Environmental Assessment and Water Research (IDAEA-CSIC), Jordi Girona 18, 08034 Barcelona, Catalonia, Spain

HIGHLIGHTS

- Gas-phase SVOC concentrations were determined in a remote high-mountain location.
- Passive sampling rate errors adequately conformed to theoretical uncertainties.
- Passive sampling concentrations showed high agreement with active air sampling ones.

GRAPHICAL ABSTRACT

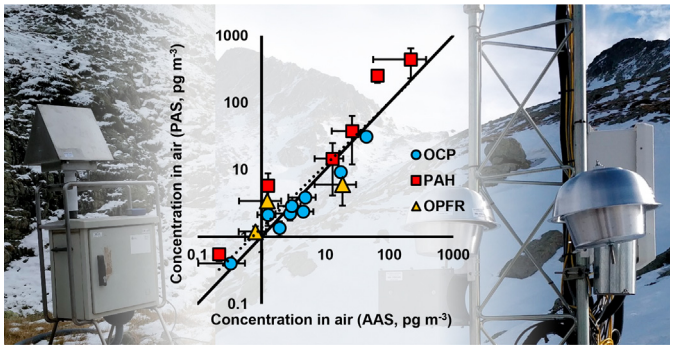

ARTICLE INFO

Article history:
Received 29 June 2021
Received in revised form 13 August 2021
Accepted 13 August 2021
Available online 21 August 2021

Editor: Shuzhen Zhang

Keywords:
Passive air sampling
Active air sampling
Semi-volatile organic compounds
Performance reference compounds
Calibration
Field comparison

ABSTRACT

Polyurethane foam passive air samplers (PUF-PAS) are good candidates for the determination of gas-phase semi-volatile organic compound (SVOC) air concentrations in high-mountain areas over long periods because they do not require an energy supply. However, the harsh meteorological conditions present in such locations can increase the uncertainties inherently associated to PAS sampling rates due to the many variables involved in their calculation and to the assumptions made regarding PUF diffusive uptake mechanics, which can considerably bias the resulting concentrations. Therefore, we studied the performance of PUF-PASs in a remote location in the Pyrenees mountain range for the analysis of several SVOCs in air, including polychlorobiphenyls (PCBs), hexachlorobenzene, pentachlorobenzene, polycyclic aromatic hydrocarbons (PAHs), and the less studied emerging organophosphate flame retardants (OPFRs). An in-situ PUF-PAS calibration using Performance Reference Compounds (PRCs) provided compound- and sampler-specific sampling rates, showing mean experimental errors (12%) that adequately conformed to an estimate of their expanded theoretical uncertainties (15%). This showcases the suitability of this calibration strategy in an area with conditions beyond those typically considered in calibration efforts available to date. Moreover, gas-phase concentrations of the studied pollutants from PUF-PAS samples showed very good agreement (R^2 up to 0.91, $p < 0.01$) when compared to those obtained using a conventional high-volume active air sampler (PUF-AAS), with some minor deviations observed for PAHs caused by the seasonality in their atmospheric concentrations. No relevant levels of pollutants preferentially bound to the particle phase were detected in the PUF-PASs, the particle infiltration efficiency of the sampler configuration used was found to be low, and compounds typically distributed between the gas and particle phases of AAS samples revealed profiles consistent with their vapor pressures, except for some OPFRs.

* Corresponding author.
E-mail address: raimon.martinez@idaea.csic.es (R.M. Prats).

https://doi.org/10.1016/j.scitotenv.2021.149738

1. Introduction

1.1. Passive air sampling calibration in high-mountain locations

High mountains and colder regions at higher latitudes tend to accumulate semi-volatile organic compounds (SVOCs), including persistent organic pollutants (POPs), that reach them through long-range atmospheric transport (Wania and MacKay, 1996; Grimalt et al., 2001). This process makes these areas reference sites for the study of the global impact of the use of chemical compounds of anthropogenic origin. At present, polyurethane foam (PUF) disks are commonly used for the analysis of these pollutants in a broad array of locations (Pozo et al., 2006; Shoeib and Harner, 2002). They are simple to use, relatively inexpensive, do not require an energy source, and are convenient for deployment over long periods. These characteristics make them good candidates for atmospheric monitoring programmes in remote and difficult to access locations, compared to the traditional active air sampling (AAS) alternatives. Moreover, they are capable of sampling a wide range of semi-volatile organic compounds; for example, these samplers have been used for the study of polychlorinated biphenyls (PCBs), organochlorine pesticides (OCPs), polybrominated diphenyl ethers (PBDEs), and other SVOCs in remote locations like Antarctica (Li et al., 2012; Pozo et al., 2017), the Tibetan Plateau (Ren et al., 2014), and high-mountain ranges in Brazil (Guida et al., 2018). They have also been shown to collect particle-associated chemicals (Harner et al., 2013; Markovic et al., 2015).

However, the conversion of adsorbed amounts of pollutants to gas-phase concentrations is not trivial, since the sampled air volumes depend on the storage capacity of the PUF, the physical-chemical properties of each SVOC, and the physical conditions of the atmosphere. Although some studies have suggested the dispensability of AAS for the assessment of long-term trends in atmospheric concentrations of certain pollutants (Kalina et al., 2017), parallel AAS measurements are often used to calibrate PAS-PUFs: PAS sampling rates are derived from short AAS sampling periods, where the amount of passively adsorbed compound is normalized to exposure time and divided by its concentration in air determined from AAS (Chaemfa et al., 2009a; Harner et al., 2013; Klánová et al., 2008; Mari et al., 2008). Yet potential problems arise from the assumptions of sampler-independent uptake rates and linear compound uptake conditions that do not always apply for all studied compounds. Moreover, AAS samples used for PAS calibration only account for a very short interval of PAS exposure time (a few hours compared to many weeks or months), bringing into question the representativeness of AAS-derived sampling rates. Secondly, the extent to which particle-phase chemicals are captured by the PUF-PAS sampler configuration can affect the true gas-phase sampling rates. Another practical obstacle is the difficulty, or impossibility, to link PAS measurements to AAS concentrations in remote locations due to difficult access and the lack of an energy supply. Alternatively, PAS sampling rates can be estimated by determining the extent of the linear uptake phase of SVOCs along long sampling periods (Abdollahi et al., 2017; Chaemfa et al., 2008; Evci et al., 2016). Studies using this PAS calibration strategy reported concentrations within a factor of two of AAS measurements for PCBs and OCPs in an urban location in South Korea (Heo and Lee, 2014), and good sampling performances with satisfactory levels of confidence were found for PCBs, OCPs, and PAHs in the Czech Republic (Bohlin et al., 2014).

However, the use of Performance Reference Compounds (PRCs, sometimes referred to as Depuration Compounds, DCs) offers a more reliable PUF-PAS calibration method (Harner et al., 2013). PRCs are a set of compounds representative of a range of physical-chemical properties similar to those of the targeted pollutants. They are spiked into the sampler upon deployment and are diffusively released from the PUF into the air at different rates. The dissipation rate of PRCs is proportional to the uptake of the target compounds (Huckins et al., 2002), and therefore the sampling rates can be estimated, but their calculation is complex and affected by uncertainties. Nevertheless, this approach eliminates the dependence of PAS on AAS measurements for the determination of compound-specific effective sampled volumes and produces sampling rates distinct for each sampler that account for the variability in physical conditions of each studied location. This is particularly useful in remote areas like high mountains, where calculating site-specific rates is of critical importance due to the extreme weather conditions. A few studies compared the performance of PRC-calibrated PAS with conventional AAS. Atmospheric POP concentrations determined using this approach were within a factor of two or three compared to those obtained by AAS in tropical environments (Gouin et al., 2008; He and Balasubramanian, 2010), and in the Great Lakes basin (Gouin et al., 2005; Hayward et al., 2010). However, to the extent of our knowledge there have been no independent comparison attempts in remote high-mountain areas.

1.2. Uncertainty in passive sampling rates

The determination of sampling rates by PRC calibration often carries considerable uncertainties, mostly associated to the multiple variables involved in the calculation of uptake rates and to the assumptions made regarding the diffusive uptake mechanics of the passive sampler medium (Herkert et al., 2018). On one hand, uptake rates have been shown to be influenced by wind speed (Klánová et al., 2008; Moeckel et al., 2009; Tuduri et al., 2006) since the renewal of air inside the sampler housing determines the thickness of the boundary layer of air that is assumed to control uptake and loss of compounds. This can introduce substantial uncertainty depending on the wind speed, the PAS housing design, and its location and orientation (Chaemfa et al., 2009b; Zhang et al., 2015). On the other hand, temperature is the driving force behind molecular diffusivity and uptake or release from the sampler material. PAS applications often benefit from temperate and stable conditions rather than those usually associated with high-mountain locations since PRC calibration takes advantage of moderate and controlled PRC release rates, although diffusivity changes due to temperature variation have been shown to have a relatively smaller impact on sampling rates over a 20 °C range (e.g., from 0 to 20 °C) compared to other factors like wind speed (Shoeib and Harner, 2002). Most PUF-PAS calibration efforts until now have thus been carried out in temperate climates and conditions (Wania and Shunthirasingham, 2020). Moreover, differences between ambient and in-housing registered temperatures can also lead to considerable error in the estimation of sampled volumes (Kennedy et al., 2010).

Therefore, the estimation of sampling rates can lead to non-negligible margins of error in the resulting atmospheric pollutant concentrations, especially in the case of remote locations such as high mountains. Nevertheless, the need for PRC calibration in such places is paramount. Some studies have previously relied on the pool of available data by averaging uptake rates and assuming equal and constant values in their measurements (Mari et al., 2008; Cheng et al., 2013; Jaward et al., 2005; Zhang et al., 2008), but this can induce greater error by not accounting for variability between samples, locations, and sampling periods. Studies in high-mountain sites and other remote areas may be biased from these assumptions more strongly, as the extreme wind velocities, strong solar irradiance, and ample temperature ranges become large sources of uncertainty that need to be accounted for. Other studies have extensively evaluated the use of PRCs and the effect of meteorology on PAS sampling rates, proposing alternative models for the estimation of effective sampled volumes using only publicly available meteorological data (Herkert et al., 2018), although it proved more difficult to interpret at higher wind speeds. However, PAS uncertainties are very rarely reported along with sampling rate estimates in the available literature, which is why the need for uncertainty appraisal has been specifically put forward (Wania and Shunthirasingham, 2020).

Accordingly, we deployed PAS and AAS samplers in a high-mountain location in the Pyrenees mountain range for the determination of gas-

phase concentrations of a wide range of SVOCs including PCBs, OCPs, polycyclic aromatic hydrocarbons (PAHs), and organophosphate flame retardants (OPFRs). The effective sampled volumes that allow the conversion of PUF adsorbed amounts to concentrations were calculated by PRC calibration, thus enabling an independent comparison with AAS measurements. The experimental errors in the sampling rates were examined in contrast to an estimate of their theoretical uncertainty in an effort to identify and quantify the main sources of error. Moreover, the agreement between AAS and PAS concentrations was assessed, providing new insight on the reliability of PUF-PAS samplers for the determination of multiple gas-phase semi-volatile pollutants in a remote high-mountain location with characteristics beyond those typically considered in the scope of similar studies (i.e., extreme meteorological conditions and very low pollutant levels).

2. Materials and methods

2.1. Sampling site

All samples were collected near Estanh Redon, a lake located in the Central Catalan Pyrenees (42°38'18.1" N, 0°46'44.1" E, 2240 m.a.s.l.). Estanh Redon is an alpine lake situated above the local tree line, with a hydrology related only to atmospheric precipitation. It has been used as an environmental and biological research site for decades because of its remoteness. The area is characterized by a broad range of temperatures (-16.6–25.1 °C during the deployment of our samples) and periods of extremely high wind speeds (up to 36.2 m s^{-1}, or 130 km h^{-1}). More detailed meteorological conditions have been summarized in Table 1, obtained at a 30 min resolution from an automatic weather station (VS station) from the Catalan Meteorological Service XEMA network located at the exact point of deployment.

2.2. Passive air sampling (PAS)

Polyurethane foam (PUF) passive samplers were deployed in duplicate over four consecutive periods between September 2017 and October 2020 (Table 1). Their durations were 297, 154, 289, and 376 days, respectively. The PUF disks (Techno Spec, Barcelona, Catalonia, Spain) measured 14 cm in diameter, 1.35 cm in thickness, with 369.5 cm^2 of surface area, and a density of 0.021 g cm^{-3}. Prior to deployment, they were thoroughly rinsed with distilled water and acetone (Merck, Darmstadt, Germany), and Soxhlet extracted with acetone and hexane (Merck) for 24 h each. They were further extracted with hexane for another 8 h, dried under vacuum, placed inside acetone-rinsed aluminium foil, sealed air-tight inside of PET/LLDPE bags (Kapak Corporation, St Louis Park, MI, USA), and stored at -20 °C until deployed. They were housed inside stainless steel domes similar to those used in other monitoring programmes (e.g., Pozo et al., 2006) for the entire duration of the sampling campaign (Fig. 1), attached 3 m above ground level to a stainless steel tower structure that holds the equipment of the meteorological station.

PAS sampling rates were determined by PRC calibration (see Section 2.7 below), spiking the PUFs with a mixture of PCB congeners 3, 9, 15, 32 (all labelled), 107, and 198 (Cambridge Isotope Laboratories, Tewksbury, MA, USA) upon deployment. After their retrieval, the PUFs were sealed again and transported in a refrigerated container and stored at -20 °C until extracted. Two field blanks were performed for each sampling period, being transported with the samples, exposed during deployment and retrieval, spiked with the PRC mixture, and stored at -20 °C for the duration of the sampling until extracted alongside the samples.

2.3. Active air sampling (AAS)

Three AAS samples were obtained in July and September 2017 (Table 1) using a high-volume air sampler (MCV, Collbató, Catalonia, Spain) placed 30 m away from the PAS samplers and connected to a gasoline-fuelled energy generator situated 50 m downwind from both sampler devices. Gas-phase samples were collected with two PUF plugs (6 cm diameter, 10 cm thickness, 0.0285 g cm^{-3} density) inside a Teflon tube, preceded by a 20.3 × 25.4 cm GF/A glass fiber filter (GFF) (Whatman, Maidstone, England) that collected the atmospheric particle phase. Samples between 125 and 242 m^3 were collected at 20 m^3 h^{-1}. The PUF-AAS plugs were pre-cleaned, transported, and stored as described for the PUF-PAS disks. The GFF filters were pre-treated in a muffle furnace at 450 °C overnight and transported and stored in the same way. Field blanks were also performed for each AAS sample by exposing PUF plugs and filters to the atmosphere during the collection of samples.

Back-trajectories of the air masses arriving at the sampling location during the collection of AAS samples were calculated for 72 h backwards using the NOAA Hysplit model (Stein et al., 2015) (Fig. S1a–c).

2.4. Extraction and clean-up

The PUF-PAS disks and the PUF-AAS plugs were Soxhlet extracted for 8 h with hexane, and the GFF-AAS filters were extracted three times by sonication for 15 min with hexane:dichloromethane 4:1 *v*/v (all solvents from Merck). The following recovery standards were spiked onto the sampler media before the extraction: 1,2,4,5-tetrabromobenzene, PCB209 (Dr. Ehrenstorfer, Augsburg, Germany), acenaphthene-d_{10}, fluorene-d_{10}, phenanthrene-d_{10}, anthracene-d_{10}, fluoranthene-d_{10}, pyrene-d_{10}, benz[*a*]anthracene-d_{12}, chrysene-d_{12}, benzo[*b*]fluoranthene-d_{12}, benzo[*ghi*]perylene-d_{12} (National Institute of Standards and Technology, Gaithersburg, MD, USA), tributyl phosphate-d_{12}, tris(2-chloroethyl) phosphate-d_{12}, tris(1-chloro-2-propyl) phosphate-d_{18}, tris(1,3-dichloro-2-propyl) phosphate-d_{15}, and triphenyl phosphate-d_{15} (Cambridge Isotope Laboratories). The extracts were concentrated to 2 mL with a vacuum rotary evaporator (Büchi, Flawil, Switzerland) and further concentrated to 0.5 mL under a gentle stream of nitrogen gas.

The clean-up of the extracts was performed by HPLC fractionation as described elsewhere (Prats et al., 2021). Briefly, an Agilent 1200 Series system (Agilent Technologies, Santa Clara, CA, USA) equipped with a preparative fraction collector and a Tracer Excel 120 SI HPLC silica column 25 cm × 3 μm × 0.46 cm i.d. (Teknokroma, Sant Cugat del Vallès, Catalonia, Spain) was used for the separation of compounds. Following the injection of 10 μL of extract, two separate fractions were collected

Table 1
Passive (PAS) and active (AAS) air sampling periods and atmospheric conditions.

	PAS I	PAS II	PAS III	PAS IV	AAS I	AAS II	AAS III
Start date	17/09/2017	11/07/2018	12/12/2018	27/09/2019	25/07/2017	26/07/2017	17/09/2017
End date	11/07/2018	12/12/2018	27/09/2019	07/10/2020	25/07/2017	26/07/2017	17/09/2017
Sampled time (d)	297	154	289	376	–	–	–
Sampled volume (m^3)	–	–	–	–	242	125	158
Average temperature (°C)	0.7	6.8	4.1	4.2	6.0	5.6	2.6
(Min–Max)	(-16.6–18.2)	(-9.2–20.3)	(-14.1–25.1)	(-16.6–23.3)	(5.7–6.4)	(5.3–5.9)	(2.4–2.9)
Average wind speed (m s^{-1})	4.7	4.4	4.8	4.6	5.4	5.6	6.6
(Min–Max)	(0–36.2)	(0–33.9)	(0–36.0)	(0–35.6)	(2.9–12.1)	(3.9–12.4)	(2.0–13.2)

Fig. 1. PUF-PAS samplers deployed in the Pyrenees (2240 m.a.s.l.) inside dome-style stainless steel housings affixed to the structure of an automatic weather station.

after an initial elution of 8 min of 100% hexane at 0.5 mL min^{-1}: a first one for PCBs and OCPs (min 8–15 while performing a solvent composition gradient to 20% dichloromethane) and a second one for PAHs (min 15–20 maintaining solvent composition). The fractions were then concentrated under a stream of nitrogen gas. OPFRs were analysed without requiring HPLC fractionation after drying an aliquot of the original extract through 0.5 g of anhydrous sodium sulphate (Merck) activated at 450 °C in a muffle furnace.

2.5. Instrumental analysis

The extract fractions were injected into a gas chromatograph coupled to a mass spectrometer (GC–MS). A targeted analysis was performed for the following compounds: PAHs, acenaphthene (ace), fluorene (fle), phenanthrene (phe), fluoranthene (flu), pyrene (pyr), benz[*a*]anthracene (b[*a*]ant), chrysene+triphenylene (chr + triph), benzo[b], [j], and [k]fluoranthenes (b[b + j + k]flu), benzo[*e*]pyrene (b[*e*]p), benzo[*a*]pyrene (b[*a*]p), indeno[1,2,3-*cd*]pyrene (ind[123 *cd*]pyr), and benzo[*ghi*]perylene (b[*ghi*]pery); PCB congeners 28, 52, 101, 118, 138, 153, and 180; and OCPs hexachlorobencene (HCB) and pentachlorobenzene (PeCB). They were identified in SIM mode by retention time and *m*/*z* ratios (Table S1). A Thermo Trace GC Ultra–DSQ II (Thermo Fisher Scientific, Waltham, MA, USA) GC–MS system was used, with a 60 m × 0.25 mm i.d. × 25 μm HP-5MS fused capillary column (Agilent Technologies) in electron impact mode at 70 eV. The injector, ion source, quadrupole, and transfer line temperatures were 280, 250, 150, and 270 °C, respectively. Helium was used as carrier gas (1 mL min^{-1}). The oven program was as follows: 90 °C (1 min) to 150 °C at 10 °C min^{-1} and to 320 °C at 6 °C min^{-1}, with a final holding time of 20 min.

The following OPFRs were analysed by GC coupled to tandem mass spectrometry (GC–MS/MS): tributyl phosphate (TBP), tris(2-chloroethyl) phosphate (TCEP), tris(1-chloro-2-propyl) phosphate (TCPP), tris(1,3-dichloro-2-propyl) phosphate (TDCP), and triphenyl phosphate (TPhP). They were identified in MRM mode by retention time and one quantifier and one qualifier *m*/*z* transitions (Table S2). An Agilent 7000 Series Triple Quad GC/MS (Agilent Technologies) system was used, with a 30 m × 0.25 mm i.d. × 0.25 μm Zebron ZB-PAH capillary column (Phenomenex, Torrance, CA, USA) in electron impact mode. The injector, ion source, quadrupoles, and transfer line temperatures were 280, 230, 150, and 280 °C, respectively. Helium was used as a carrier gas at 1.1 mL min^{-1}. The oven program was as follows: 80 °C (1.5 min) to 220 °C at 10 °C min^{-1} and to 315 °C at 15 °C min^{-1}, with a final holding time of 5 min.

2.6. Quality control and assurance

At least one field blank per sampling was performed as described above, taking meticulous measures to avoid contamination of the samplers in the field, during transport, and in the laboratory. They were transported, stored, extracted, and analysed along with each batch of samples. Average blank levels were subtracted from the pollutant amounts in each sampler. Special care was put into avoiding contamination from the exhaust of the energy generator used for AAS sample collection, which was placed over 50 m downwind from the sampler. PAH levels in AAS blanks were compared to PAS blanks in search of increased levels due to exhaust fumes, as observed in previous studies (Fernández et al., 2002), and no influence of such contamination was detected.

Breakthrough of gas-phase pollutants in the PUF-AAS sampling has been previously studied using the same equipment we used, in very similar conditions and at the same site (Fernández et al., 2002; van Drooge et al., 2002). Compounds that can be affected by breakthrough tend to be those with higher volatilities such as naphthalene, acenaphthylene, or pentachlorobenzene, so this was considered when choosing the set of targeted compounds.

The quantification of the target pollutants was performed by internal standard calibration, which accounts for extraction and processing recoveries as well as for analysis variability. Recoveries of most surrogate standards ranged between 73 ± 24% and 103 ± 18% for deuterated PAHs, with the more volatile Ace-d_{10} occasionally presenting lower values or non-quantifiable peaks, between 66 ± 9% and 90 ± 28% for PCBs and OCPs, and between 48 ± 11% and 106 ± 10% for OPFRs, with TDCP occasionally presenting lower values or non-quantifiable peaks due to interferences. In-column limits of quantification ranged between 0.5 and 2.5 pg, or 25 to 125 pg $sampler^{-1}$ for PAHs and OCPs, and 0.12 to 0.25 pg in-column or 6.25 to 12.5 pg $sampler^{-1}$ for OPFRs. For average PAS effective sampled volumes, these translate to instrumental LOQs of 0.1–0.4 pg m^{-3} for PAHs and OCPs and 0.01–0.03 pg m^{-3} for OPFRs. For average AAS sampled volumes, they are 0.1–0.7 pg m^{-3} for PAHs and OCPs and 0.04–0.07 pg m^{-3} for OPFRs.

2.7. Determination of PAS concentrations

Concentrations of gas-phase pollutants in air (C_A, pg m^{-3}) were calculated by determining compound- and sample-specific effective sampled air volumes (V_A, m^3). These are theoretical volumes of air by which the amount of compound found in the PUF-PAS samplers (pg $sampler^{-1}$) was divided in order to provide an estimate of C_A, accounting for differences both in sampling conditions between periods and in physical-chemical properties between compounds. Here, V_A were calculated as follows (Harner et al., 2013):

$$V_A = V_{PUF}\, K\prime_{PUF-A}\left[1 - exp\left(\frac{-k_A\, t}{K\prime_{PUF-A}\, D_{film}}\right)\right] \quad (1)$$

where V_{PUF} is the volume of the PUF disk (m^3), k_A is the sample-specific air-side mass transfer coefficient (m d^{-1}), t is the duration of the sampling campaign (d), D_{film} is the effective film thickness of the PUF disk (0.00567 m), and $K'_{PUF\text{-}A}$ is the density-corrected PUF-air partition coefficient (unitless) calculated by multiplying $K_{PUF\text{-}A}$ (m^3 g^{-1}) by the density of the PUF (g m^{-3}). $K_{PUF\text{-}A}$ values depend on the sampler material and are compound-specific. They were calculated from octanol-air partition coefficients (K_{OA}) as $\log K_{PUF\text{-}A} = 0.6366 \times \log K_{OA}$

– 3.1774 (Shoeib and Harner, 2002). Temperature-corrected K_{OA} values for the studied compounds were obtained from temperature dependence correlations reported in other studies (Chen et al., 2016; Harner, 2021; Odabasi et al., 2006; Wang et al., 2017). Although this $K_{PUF\text{-}A}$–K_{OA} relationship has been extensively used for many SVOCs, recent reports argued that compounds like OPFRs may behave quite differently (therefore making the previous equation not accurate for the estimation of sampled volumes) and proposed a new relationship (Saini et al., 2019). This could lead to added uncertainty on OPFR atmospheric concentrations, so the newly proposed equation ($\log K_{PUF\text{-}A} = 0.6087 \times \log K_{OA} + 2.3821$) was also used for comparison.

The calculation of k_A transfer coefficients involves the calibration of each sampler in situ. This is often done by determining sampling rates (R_S, $m^3\ d^{-1}$) for each individual sampler using PRCs. The dissipation rate of PRCs is proportional to the uptake of the target compounds, and therefore to their mass transfer coefficients (Huckins et al., 2002). They were calculated as follows:

$$k_A = \frac{R_S}{A_{PUF}} = \frac{\ln(C/C_0)\, K\prime_{PUF-A}\, D_{film}}{t} \quad (2)$$

where A_{PUF} is the area of the PUF disk (m^2), and where PRC release ratios are defined as the amount of each PRC left in the exposed sampler after its retrieval (C) divided by the amount found in the field blanks (C_0). These PRC relative amounts were also corrected for recovery and for instrumental variability using the internal standards added before the extraction of the respective exposed and blank PUFs.

The theoretical uncertainty of R_S was estimated through the error propagation of the non-constant variables and coefficients involved in Eq. (2). A more detailed explanation of this calculation can be found in the Supplementary Material (Text S1). Briefly, the main sources of error reside in the calculation of C/C_0 ratios and in the K_{OA} values of PRCs used for the calculation of $K_{PUF\text{-}A}$, the uncertainties of which were reported elsewhere (Harner and Bidleman, 1996). Expanded uncertainties (calculated as twice the regular uncertainty) should then confidently encompass other sources of error such as those inherent to the $K_{PUF\text{-}A}$–K_{OA} and K_{OA}–T correlations.

3. Results and discussion

3.1. PAS sampling rates and uncertainty

Table 2 summarizes the sampling rates calculated by PRC calibration of the PAS samplers for all four passive sampling periods detailed in Table 1. The mean R_S of all samplers was 3.7 ± 0.5 $m^3\ d^{-1}$, with individual replicates ranging from 2.6 to 4.5 $m^3\ d^{-1}$. This is in excellent agreement with most values in the literature and results from global PAS networks using PUF-PAS samplers with the stainless-steel dome design, which typically report R_S of 3 to 4 $m^3\ d^{-1}$ and standard deviations around 1 to 2 $m^3\ d^{-1}$ (Herkert et al., 2018; Pozo et al., 2009). Other studies in mountain locations reported PRC-derived R_S of 4.3 ± 1.6 $m^3\ d^{-1}$ in the Tibetan plateau (Ren et al., 2014), 2.7 ± 1.1 $m^3\ d^{-1}$ in the Andes (Estellano et al., 2008), and 3.6 ± 2.0 $m^3\ d^{-1}$ in southern Brazil (Meire et al., 2012). Sampling rates have often been correlated with meteorological variables such as wind speed (Klánová et al., 2008; Herkert et al., 2018). However, no significant relationship was found between our results and the average wind speeds or temperatures. This was attributed to a small number of representative sampling periods and to the average values of such variables remaining reasonably stable throughout all sampling campaigns regardless of the time of the year (0.7–6.8 °C, 4.4–4.8 m s^{-1}), despite temperature and wind speed ranges being characteristically extreme as expected in an alpine site (-16.6–25.1 °C, 0.0–36.2 m s^{-1}) (Table 1).

Table 2
Mean sampling rates (R_S) and standard deviations (SD) of passive air samplers calculated by PRC calibration, and their experimental and theoretical uncertainties.

	Mean R_S ± SD ($m^3\ d^{-1}$)	Experimental error[b]	Expanded theoretical uncertainty[c]
PAS I	3.8 ± 0.1	1.8%	15.5%
PAS II	3.2 ± 0.7	23.0%	19.4%
PAS III	3.6 ± 0.4	11.5%	15.1%
PAS IV	4.5[a]	–	10.7%
Mean	3.7 ± 0.5	12.1 ± 10.6%	15.2 ± 3.5%

[a] One duplicate was lost due to extreme weather conditions.
[b] Relative standard deviation of the duplicates.
[c] Calculated as twice the error propagated from the uncertainty in the variables used for R_S estimation.

The experimental error of R_S was calculated as the relative standard deviation of the replicates. It averaged 12 ± 11%, being as high as 23% for one of the sampled periods (Table 2). R_S could only be calculated for three of the four periods because one of the duplicates was lost due to extreme weather and wind conditions. Nevertheless, an average experimental variability below 20% is adequate considering that all R_S were within the range of typically reported values. Moreover, some differences between samplers may not be solely associated to the inherent uncertainty in the estimation of R_S, but also to differences in air flow through the PUFs due to slight deformations that resulted in tilted sampler housings after heavy snow and intense wind events. This may also explain why the experimental error in the first sampling period (PAS I), when the sampler devices were newly installed, was much smaller (< 2%) than in ensuing periods (Table 2). These differences in air flow are nonetheless accounted for when reporting pollutant concentrations because sampling rates are calculated and used independently for each replicate instead of as a period average.

Theoretical expanded uncertainties of R_S were calculated for each sampler from a rearranged Eq. (2) (see Text S1 in the Supplementary Material). They averaged 15 ± 4%, ranging from 11 to 19% (Table 2). The two main variables contributing to this uncertainty are K_{OA} and the PRC release ratios, C/C_0. K_{OA} error accounted for 68% of the total unexpanded theoretical uncertainty on average, while C/C_0 error accounted for the remaining 32%. A smaller contribution of the latter term was expected since the determination of C/C_0 does not involve particularly severe error-inducing operations, yet it still amounted to a sizeable fraction of the total uncertainty because small variations in such ratios may render substantial fluctuations in the resulting R_S. On the other hand, uncertainties of PRC K_{OA} values ranging from 2 to 35% (Harner and Bidleman, 1996) are sufficiently large to become the main source of error. This uncertainty is inherent to determining K_{OA} values and is added to that of their temperature dependence relationships and to that of the empirical regression through which $K_{PUF\text{-}A}$ is calculated (Shoeib and Harner, 2002), which were indirectly accounted for by calculating the expanded uncertainties.

An additional consideration must be made in regard to sampling rates and effective sampled volumes of OPFRs. As mentioned in Section 2.7, alternative associations between $K_{PUF\text{-}A}$ and K_{OA} have been proposed (Saini et al., 2019) arguing that some compound groups may not adequately adhere to the relationship originally described by Shoeib and Harner (2002) due to their different partitioning behavior. Therefore, we compared effective sampled volumes for OPFRs estimated using both equations (Table S3). OPFRs with higher K_{OA} values (i.e., TCPP, TDCP, and TPhP) saw very little or no change in their mean estimated volumes since they remained in the linear phase of uptake by the PUF-PAS. On the other hand, TCEP and TBP, with lower K_{OA}, presented volumes 18 and 30% lower on average using the original relationship, respectively. This is due to one order of magnitude higher $K_{PUF\text{-}A}$ values resulting from a higher intercept in the equation proposed by Saini et al. (2019), which undoubtedly adds to the overall uncertainty in OPFR measurements and must be considered when passive sampler-derived concentrations are reported. However, this equation only relies on three non-chlorinated OPFRs, and we did not consider the resulting differences to be large enough to adopt

the newest equation just for two compounds. This also allows for direct comparison with other previously reported concentrations.

Overall, the average experimental variability observed in the sampling rates adequately fits within the mean estimated expanded uncertainty. However, this does not always need to be the case. Factors beyond the purely theoretical and analytical ones considered for the calculation of the uncertainty can induce pronounced disagreements between sample replicates (e.g., sampler housing inclination causing differences in wind flux through the samplers). Nevertheless, the fact that they both remained confidently below 20% illustrates the suitability and reliability of our PAS measurements. Still, an uncertainty of up to 20% could potentially translate into misjudgements of effective sampled volumes of 100–200 m^3 on average. Therefore, we performed an in-situ field comparison between PUF-PAS and PUF-AAS sampling techniques for further assessing the accuracy of PAS measurements.

3.2. Comparison between PAS and AAS

The degrees of equilibrium (DEQ) reached by the studied compounds during the exposure of each PUF-PAS were calculated as a measure of the performance of these passive samplers across all sampling campaigns in this study and are summarized in Table S4. The DEQ is the magnitude to which the uptake of a compound by the PUF-PAS departed the linear regime and approached equilibrium between air and the PUF. They can be obtained from the components between brackets in Eq. (1). As expected, the more volatile compounds (i.e., PAHs Ace, Fle, and Phe; OCPs PeCB and HCB) reached near or complete equilibrium during all sampling campaigns (DEQ close to 1). They were followed by the low molecular weight PCB28 and the lowest K_{OA} OPFRs TBP and TCEP (mean DEQ between 0.32 and 0.50). All other compounds had low DEQs (below 0.29) signifying a still close-to-linear uptake regime, especially for OPFRs with the highest K_{OA} (DEQ almost 0). This reflects the usefulness of a complete PRC calibration of individual PUF-PASs for studies encompassing a set of compounds with a wide range of physical-chemical properties. Otherwise, the assumption of an invariable linear uptake would lead to a large overestimation of atmospheric concentrations of pollutants that tend to equilibrate more easily.

Table 3 contains the mean gas-phase concentrations obtained using both AAS and PAS methods, along with their standard deviations. The complete results for all replicates can be found in the Supplementary Material (Table S5). Notice that the mean and standard deviation of all samples are presented for AAS, while for PAS they are the mean and standard deviation of the period averages. The agreement between PAS replicates was adequate, averaging relative standard deviations (RSD) between samplers of 23%. These mean differences were consistent for all groups of analysed compounds, with the unique exception of TPhP resulting from a local contamination (see Section 3.4). AAS concentrations were relatively similar between samples, considering their different sampling periods (mean RSD of 41%). Concentrations of OCPs and PCBs were the closest between periods (RSD 33%), while OPFRs were less consistent (59%). It is worth noting that the AAS concentrations of many pollutants in the first sampling period (AAS I) were frequently higher than in the following ones (Table S5). A possible explanation resides in the origin of air mass trajectories computed backwards for each AAS period (Fig. S1). While all of them have a North-Atlantic origin, the trajectories for AAS I have a more pronounced continental component and lower altitudes that may have increased the levels of pollutants they carried.

AAS and PAS mean concentrations were compared to each other to determine the accuracy and suitability of PRC-derived concentrations. Fig. 2 displays the correlation between results from both methods, shown for average PAS results and for the PAS campaign closest to the collection of AAS samples (PAS I). Overall, an adequate linear correlation was observed between measurements (R^2 0.86, $p < 0.01$), showing even better goodness of fit when only PAS I was considered (R^2 0.91, $p < 0.01$). This improvement is a result of PAS campaigns representing much longer sampling periods that encompassed different seasons, which usually induces higher variability in the results. Alternatively, a power regression was adjusted to the data and is shown in Fig. 2, which better represents the closeness of the data to the identity line. In general, agreement between values factoring in their standard deviations indicates the capability of PUF-PAS samplers to replicate the results of the reference PUF-AAS values.

Table 3
Mean gas-phase concentrations and standard deviations (SD) of target organic pollutants determined using passive air sampling (PAS, $n = 4 \times 2$ replicates) and active air sampling (AAS, $n = 3$) methods. Particle-phase concentrations are shown for the active sampling glass fiber filters (GFF-AAS), along with the fraction of compounds distributed in the particle phase over their total concentration (gas + particle) and their log-transformed octanol-air partition coefficients ($\log K_{OA}$) at 25 °C.

	PUF-PAS		PUF-AAS		GFF-AAS			$\log K_{OA}$
	pg m^{-3}	SD	pg m^{-3}	SD	pg m^{-3}	SD	Part %	
HCB	36	16	44	2.5	n.d.[a]	–	–	7.4
PeCB	21	19	17	2.1	n.d.	–	–	6.2
PCB28	4.5	3.5	1.9	0.3	n.d.	–	–	7.9
PCB52	2.5	1.5	1.3	0.4	n.d.	–	–	8.4
PCB101	3.7	1.4	4.8	2.2	n.d.	–	–	8.8
PCB118	2.2	1.1	4.5	2.0	n.d.	–	–	8.5
PCB153	2.5	0.6	2.8	1.1	n.d.	–	–	8.5
PCB138	2.1	1.1	3.0	1.1	n.d.	–	–	8.5
PCB180	1.1	0.7	0.3	0.2	n.d.	–	–	9.1
ΣPCB_{gas}	19		19					
Ace	28	18	11	7.1	n.d.	–	–	6.1
Fle	276	50	65	1.5	4.1	1.8	6%	6.2
Phe	388	102	216	160	n.d.	–	–	7.0
Flu	60	25	26	14	7.7	6.2	24%	8.4
Pyr	24	14	13	6.1	9.1	2.3	33%	8.4
B[*a*]ant	0.8	0.4	0.2	0.03	1.9	1.7	85%	9.2
Chry + TriPh	9.7	7.0	1.3	0.02	2.6	3.9	42%	9.2
ΣPAH_{gas}	787		332					
B[b + j + k]flu	n.d.	–	n.d.	–	6.3	–	100%	10.6
B[*a*]pyr	n.d.	–	n.d.	–	1.0	1.5	100%	10.6
B[*e*]pyr	n.d.	–	n.d.	–	1.2	–	100%	10.6
Pery	n.d.	–	n.d.	–	0.2	–	100%	10.6
Db[*ah*]ant	n.d.	–	n.d.	–	0.2	–	100%	11.4
Ind[123 *cd*]pyr	n.d.	–	n.d.	–	2.0	3.0	100%	12.0
B[*ghi*]pery	n.d.	–	n.d.	–	4.7	4.0	100%	12.6
ΣPAH_{part}					42			
TBP	1.2	1.0	0.8	0.4	28	26	96%	7.6
TCEP	7.8	10	1.2	0.8	189	125	99%	8.0
TCPP	16	7.0	18	12	32	24	61%	9.7
TDCP	2.1	0.9	n.d.	–	2.9	1.2	99%	10.6
TPhP	2063[b]	2840[b]	0.3	0.3	11	5.3	97%	10.9
$\Sigma OPFR_{gas}$	27[c]		20[c]					
$\Sigma OPFR_{part}$					263			

[a] Not detected (below detection limit or below blank levels).
[b] Affected by a local contamination (see Section 3.4).
[c] TPhP not included.

Total PCB concentrations (ΣPCB_{gas}) were 19 pg m^{-3} for both AAS and PAS samples (Table 3), revealing a very good agreement between methods. Concentrations of individual congeners ranged between 0.3 and 4.8 pg m^{-3}, with comparable composition profiles except for a 2.4 times higher PAS concentration of the most volatile PCB28. Nevertheless, this difference is still well within other reported disagreement factors for PCBs (Heo and Lee, 2014; Bohlin et al., 2014; Gouin et al., 2005), and a strong correlation was observed between both methods (Fig. 2). Mean HCB and PeCB concentrations determined using both techniques were also comparable: 36 pg m^{-3} (PAS) and 43 pg m^{-3} (AAS) for HCB, and 21 pg m^{-3} (PAS) and 17 pg m^{-3} (AAS). This level of agreement was similar or better than those reported in other studies (Gouin et al., 2008; Hayward et al., 2010). In general, ΣPCB_{gas} and individual congener concentrations were on the lower range of values reported in the same area two decades ago (16–70 pg m^{-3}), while HCB (49 pg m^{-3}) did not suffer major changes (van Drooge et al., 2004; van Drooge et al., 2005). This demonstrates the persistence of these compounds in the environment after being banned for decades, especially in remote locations. PeCB concentrations were also similar to

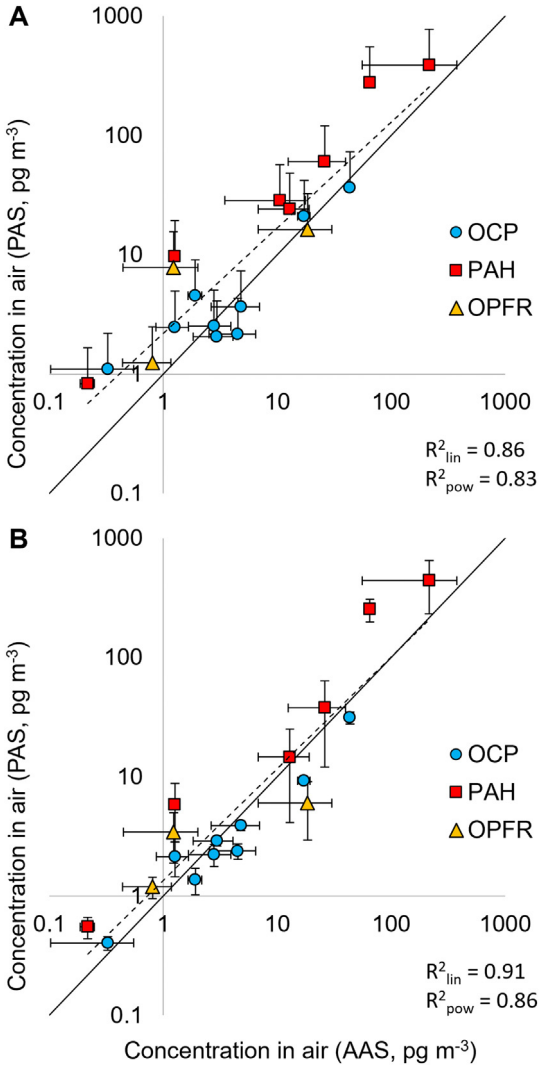

Fig. 2. Comparison of the gas-phase concentrations of organochlorine pesticides (OCP), polycyclic aromatic hydrocarbons (PAH), and organophosphate flame retardants (OPFR) determined using passive air sampling (PAS) and active air sampling (AAS) methods. Regressions are shown for A: mean of four PAS sampling periods; B: sampling period closest to the collection of AAS samples. The error bars represent standard deviations, the dashed line is a power regression for all compounds, and the continuous line represents equal PAS and AAS values.

those found in another remote mountain area in the Tibetan Plateau, 25 pg m^{-3} (Zhu et al., 2014).

The sum of mean PAH concentrations (ΣPAH_{gas}) was 332 pg m^{-3} (AAS) and 787 pg m^{-3} (PAS) (Table 3), with Phe and Fle clearly dominating the concentration profiles (20–35% and 49–65% of total PAHs, respectively). PAS-derived concentrations for all PAHs were consistently greater (3 times on average) than those calculated from AAS samples (note that PAHs fall to the left of the continuous black line that indicates equal PAS and AAS concentrations in Fig. 2). This difference factor is greater than for all other compound groups, and can still be observed even when only the PAS sampling campaign closest to the AAS sampling periods (PAS I) is considered (Fig. 2), albeit less pronounced. The reason for this is the small number of AAS samples that could only be obtained during warmer months due to limited accessibility conditions to the sampling area, and to their short duration compared to the integrative PAS samples, therefore not being able to adequately capture the temporal variability that likely exists for PAHs due to nearby alpine sources. Unlike PCBs and OCPs, PAHs tend to experience marked seasonal changes in rural and mountain regions, with higher concentrations in winter due to intermittent biomass burning (Van Drooge and Ballesta, 2009; Van Drooge and Grimalt, 2015) and a high impact of seasonal wildfires, both of which will contribute to the integrative nature of PUF-PAS measurements but not be well represented by AAS. Similarly, some disagreement in PAH concentrations was also reported elsewhere (Bohlin et al., 2014), particularly skewed by an underrepresentation of heavier PAHs. Nevertheless, some compounds like Fluo and Pyr still showed close concentrations between both methods, and an overall disagreement factor of 2 to 3 is usually regarded as acceptable for most SVOCs in the literature (e.g., Gouin et al., 2005). Compared to PAH concentrations in high-altitude regions reported elsewhere (Fernández et al., 2002; van Drooge et al., 2010), ΣPAH_{gas} was 2 to 4 times lower than those previously found in the same location (1442 pg m^{-3}), Tyrolean Alps (1792 pg m^{-3}), and Norwegian Trollheimen (1535 pg m^{-3}), much lower than those found in the Slovakian High Tatras (4421 pg m^{-3}), but higher than in the Canary Islands (187 pg m^{-3}). In any case, the PAH composition profiles generally resembled those reported in these locations.

Finally, total OPFR concentrations ($\Sigma OPFR_{gas}$, calculated only for TBP, TCEP, and TCPP) were 20 pg m^{-3} (AAS) and 27 pg m^{-3} (PAS). TDCP and TPhP were not included because the former was not found in AAS samples above detection limits, and the latter suffered from local contamination in the PAS samples (see Section 3.4). Compound profiles were dominated by TCPP (64–90% of total OPFRs). While concentrations of TBP and TCPP between methods were in agreement, that of TCEP was more than 6 times higher in PAS on average due to a particularly high amount observed in one of the sampling periods (PAS II). When treated as an outlier, TCEP PAS concentrations were only 2 times greater on average. Nevertheless, Fig. 2 shows that none of these differences represented a large discrepancy between methods. No AAS–PAS comparison studies for OPFRs were found in the literature, and gas-phase concentrations in remote or high-mountain locations are scarcely reported. Still, our results were reasonably lower than those found in the Great Lakes (Abdollahi et al., 2017; Salamova et al., 2013), in Finland (Marklund et al., 2005), and all across Central and South America (Rauert et al., 2016).

3.3. Particle phase partitioning and PAS infiltration

The GFF-AAS filters that captured the particle phase before passing through the PUF-AAS plugs were analysed for the study of particle-associated SVOCs. PCBs and OCPs were not detected at relevant concentrations above the blanks, which is consistent with the low gas-phase concentrations observed and with previous results showing that these compounds predominantly exist in the gas phase (> 90%) (Yeo et al., 2003). Contrarily, several PAHs and OPFRs were found in the particle phase (Table 3). Detected PAHs included some of those also found in the gas-phase samples, as well as higher molecular weight PAHs usually associated to atmospheric particles. The sum of the average particulate PAH concentrations (ΣPAH_{part}) was 42 pg m^{-3}, which is similar to the one found in a previous study at the same site, 53 pg m^{-3} (van Drooge et al., 2010). However, we could not establish the presence of some more volatile PAHs like Phe and Ant in the particulate phase above blank levels. PAHs only detected in the particulate phase amounted to 37% of ΣPAH_{part}, a somewhat lower proportion than those previously reported (at 39–49%) (van Drooge et al., 2010). Regarding OPFRs, they were prominently found in the particle phase, with a sum of average particulate OPFR concentrations ($\Sigma OPFR_{part}$) of 263 pg m^{-3}. This represents a partitioning towards the particulate phase of more than 92% over total OPFR concentrations (gas + particulate), which is consistent with previous considerations indicating that OPFRs mainly exist in the particle-bound form (Abdollahi et al., 2017). The lower proportion of TCEP found in the particulate phase is consistent with the higher vapor pressures of this compound (Okeme et al., 2018), although this distribution was not observed for TCPP which has a similar vapor pressure.

Log-transformed particle to gas concentration ratios were plotted against $\log K_{OA}$ values for compounds detected in both phases (Fig. 3). A linear correlation (R^2 0.85, $p < 0.01$) was observed for most compounds. The slope of the regression (0.74) was very similar to those calculated from reported gas and particle concentrations of pollutants subject to atmospheric transport towards four continental high-mountain locations (0.64–0.75) (van Drooge et al., 2010), including the same area presented in this work (0.72). However, TCPP and TBP exhibited higher concentrations in the particulate phase than expected from their K_{OA} (Table 3), so they were not considered in the regression. Such discrepancies between experimental and K_{OA}-modelled partition ratios have been observed for the more volatile OPFRs before, with suggestions of filter-air partitioning artifacts as a possible cause (Okeme et al., 2018), although we did not observe them for TCEP. Overall, these mixed results should encourage further field studies to experimentally determine OPFR phase distributions based on their physical-chemical properties, since OPFRs are emerging pollutants that encompass a very wide range of volatilities (Sühring et al., 2016).

Finally, the passive sampling theory and all calculations regarding R_S apply only to the fraction of compounds in the gas phase. However, atmospheric particles have been shown to infiltrate into the sampler housings and remain retained by the PUF (Chaemfa et al., 2009b), and there are reports on PUF-PAS sampling of compounds typically bound to particles (Bohlin et al., 2014; Harner et al., 2013; Pozo et al., 2015). The particle infiltration efficiency of passive samplers has been shown to vary greatly for different housing configurations (Markovic et al., 2015). Here, levels of SVOCs typically associated with atmospheric particles, like PAHs with a high number of fused rings, were generally not detected in PAS samples above limits of detection or blank levels, which hints at a low particle infiltration efficiency of the housing configuration used. An approximation of such efficiency was estimated from our experimental data as $\phi_{R,P}$ ($R_{S,part}/R_{S,gas}$), the particle-phase sampling rate as a fraction of the gas-phase sampling rate. It was calculated as outlined elsewhere (Holt et al., 2017). Briefly, the studied compounds were classified as gas-phase compounds if >70% of their total concentration was found in the atmospheric gas phase of AAS samples, and particle-phase compounds if >70% was found in AAS filters (Table 3). Compounds that were infrequently detected or close to limits of detection (Ace, TDCP), outside the established thresholds (Pyr, Chr + TriPh), and with contamination (TPhP) were not considered. Average sampling rates of each group were calculated as the amount of compound in the PUF-PAS sampler divided by the average AAS bulk concentration (gas+particle) and normalized by the sampling duration. The mean $\phi_{R,P}$ was 0.23, or a particle infiltration of 23% compared to the AAS system. This efficiency was 16% if only the PAS campaign closest to the AAS measurements is considered. Note that these values may present substantial uncertainties resulting from a low amount of AAS samples, the disagreement in PAH concentrations between AAS and PAS due to seasonality, and possible artifacts from a small number of particle-phase compounds detected in the PUF-PASs or from PCBs and OCPs not being detected above blank levels in AAS filters. Still, the particle infiltration efficiency calculated only from compounds detected in both gas and particle phases (PAHs in the PAS campaign closest to AAS sampling, and OPFRs) was 18%. While a more comprehensive study would be needed to determine accurate efficiencies, these values indicate a reduced particle infiltration compared to other sampler configurations (Markovic et al., 2015). This suggests that the sampler housing used here may have acted as an effective wind shield, can explain why no correlation was found between average wind speeds and mean sampling rates. Thus, the PUF-PASs performed mainly as gas-phase samplers, which diminishes the need for effective sampled volume correction and is also an advantage in high-mountain areas, ensuring that extremely high wind speeds (up to 36 m s^{-1}, or 130 km h^{-1}, Table 1) did not impact the performance of the sampler.

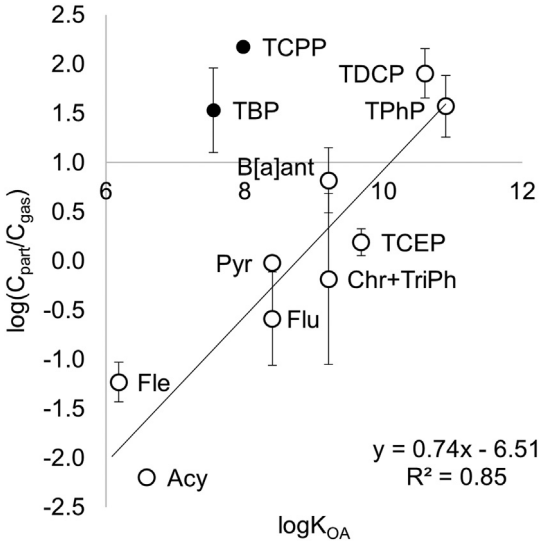

Fig. 3. Correlation between the log-transformed ratio of concentrations between pollutants in particle (Cpart) and gas (Cgas) phases and logKOA, where TCPP and TBP were not included in the regression. Error bars represent standard deviations.

3.4. Local OPFR contamination

One of the OPFRs (triphenyl phosphate, TPhP) was found in all PUF-PAS replicates at unusually high and fluctuating concentrations, averaging around 2000 pg m^{-3} (Table 3). However, it was never detected above 0.6 pg m^{-3} in AAS samples, the results of which did otherwise generally agree with those of PAS as discussed in Section 3.2. The PAS result was hypothesized to reflect a local contamination, probably due to the presence of a research cabin and meteorological station close (10 m) to the PAS deployment position (Fig. S2). In contrast, the AAS samples were collected further away (nearly 50 m) from the cabin. In order to locate the origin of such contamination, five surface soil samples were collected around the cabin and station, in addition to two samples of different insulating foams used in the interior of the cabin and between the composite metal panels that form its outer walls. They were extracted with acetonitrile after the addition of internal standards and analysed by GC–MS/MS for a quick and qualitative assessment of their OPFR composition.

Abundancies of the targeted OPFRs in each of the samples relative to the internal standards added before their extraction clearly revealed that the origin of TPhP was the insulating material used in the outer wall panels of the cabin (Fig. S3). TPhP was the dominating OPFR in this material (> 99%), while in the soil samples it only amounted to 43% on average. The second main component was TCPP, present at an abundance one to two orders of magnitude higher than in the soil samples, although amounting to only 0.3% of total OPFRs. Contrarily, the sample of inner insulation foam revealed a higher presence of TCPP (> 99%), followed by TDCP and TCEP (both around 0.2%, but still with abundancies two to three orders of magnitude higher than in the soil samples). However, no evidence of TCPP contamination was found in the PAS samples, indicating a small or negligible release rate from the interior of the cabin towards the outside. Finally, TPhP was present in the soil samples in a greater proportion than in the reference AAS samples, indicating the possible influence of this local contamination not only in air but also on the ground, but no clear pattern was observed when factoring in the distance from the source at which each soil sample was taken.

OPFRs are emerging pollutants often used as flame retardants and plasticizers in construction materials and household products. They tend to leach from such materials as they are not chemically bound and are highly susceptible to volatilization (van der Veen and de Boer,

2012). The presence of this local TPhP contamination, although unfortunate for the comparison of AAS and PAS presented in this study, highlights the capacity of the PUF samplers for sequestering this kind of emerging and less studied contaminants in the gas phase notwithstanding their tendency to associate to atmospheric particles (Abdollahi et al., 2017). However, it also exposes the impact that unexpected anthropogenic influences can have on atmospheric pollution studies, especially in areas with low concentrations, and emphasizes the need for adequate treatment of samples and careful data interpretation. It also highlights the importance of adequate site selection and sampler placement for air monitoring studies that include currently used commercial chemicals such as flame retardants and plasticizers, extensively used as material additives, as any nearby objects or structures could greatly influence the results. Although this can be more easily preventable in remote areas such as the one in this work, special attention should be paid to avoiding adjacent sources of contamination in populated and urban environments. Furthermore, studies comparing PAS and AAS measurements should also consider the need for the highest proximity between both samplers, since our results show that cases of local contamination could be inadequately reflected in the samples even by being separated only by a few tens of meters.

4. Conclusions

Polyurethane foam passive air samplers (PUF-PAS) are a useful method for the determination of gas-phase semi-volatile organic compounds in high mountain areas. Their calibration using Performance Reference Compounds (PRCs) produces compound- and sampler-independent sampling rates that account for spatial, temporal, and meteorological differences between samples. The experimental variability observed between the sampling rates of our PAS samples adequately conforms to the estimates of their expanded theoretical uncertainties. On average, sampling rate uncertainties were well below 20%, indicating an adequate precision of the PRC calibration of the PUF-PASs. A comparison of PAS-derived gas-phase concentrations with high-volume active air samples (AAS) showed good agreement between both techniques for different semi-volatile pollutants subject to long-range atmospheric transport at low concentrations. This includes pollutants like PCBs, HCB, PeCB, PAHs, and the less studied emerging OPFRs. These results showcase the suitability of PUF-PAS samplers for the monitoring of SVOCs in remote high-mountain locations with typically low pollutant concentrations and extreme atmospheric and meteorological conditions. Finally, the distribution of most compounds found both in the gas and particle phases of AAS samples revealed profiles consistent with their vapor pressures, except for some OPFRs with higher particle phase concentrations than anticipated. No relevant levels of pollutants typically bound to the particle phase were detected above limits of detection or blank levels in the PUF-PASs.

CRediT authorship contribution statement

RP: sampling, analysis, formal analysis, visualization, and writing – original draft. BD: sampling, analysis, supervision, and writing – review and editing. PF: supervision, writing – review and editing. JG: conceptualization, writing – review and editing, and funding acquisition.

Declaration of competing interest

The authors declare that they have no known competing financial interests or personal relationships that could have appeared to influence the work reported in this paper.

Acknowledgements

Sampling support from Alejandro G. Inarra and Anna Canals-Angerri, and technical assistance from Roser Chaler are acknowledged. The NOAA Air Resources Laboratory (ARL) is acknowledged for the provision of the HYSPLIT transport and dispersion model and READY website.

Funding

This work was supported by the Spanish Ministry of Science and Innovation (CTM2015-71832-P and PGC2018-102288-B-I00). Raimon M. Prats also acknowledges financial support from the Spanish Ministry of Science and Innovation (BES-2016-076339).

Appendix A. Supplementary data

Supplementary data to this article can be found online at https://doi.org/10.1016/j.scitotenv.2021.149738.

References

Abdollahi, A., Eng, A., Jantunen, L.M., Ahrens, L., Shoeib, M., Parnis, J.M., Harner, T., 2017. Characterization of polyurethane foam (PUF) and sorbent impregnated PUF (SIP) disk passive air samplers for measuring organophosphate flame retardants. Chemosphere 167, 212–219. https://doi.org/10.1016/j.chemosphere.2016.09.111.

Bohlin, P., Audy, O., Škrdlíková, L., Kukucka, P., Pribylová, P., Prokeš, R., Vojta, Š., Klánová, J., 2014. Outdoor passive air monitoring of semi volatile organic compounds (SVOCs): a critical evaluation of performance and limitations of polyurethane foam (PUF) disks. Environ. Sci. Process. Impacts 16, 433. https://doi.org/10.1039/c3em00644a.

Chaemfa, C., Barber, J.L., Gocht, T., Harner, T., Holoubek, I., Klanova, J., Jones, K.C., 2008. Field calibration of polyurethane foam (PUF) disk passive air samplers for PCBs and OC pesticides. Environ. Pollut. 156, 1290–1297. https://doi.org/10.1016/j.envpol.2008.03.016.

Chaemfa, C., Barber, J.L., Kim, K.S., Harner, T., Jones, K.C., 2009a. Further studies on the uptake of persistent organic pollutants (POPs) by polyurethane foam disk passive air samplers. Atmos. Environ. 43, 3843–3849. https://doi.org/10.1016/j.atmosenv.2009.05.020.

Chaemfa, C., Wild, E., Davison, B., Barber, J.L., Jones, K.C., 2009b. A study of aerosol entrapment and the influence of wind speed, chamber design and foam density on polyurethane foam passive air samplers used for persistent organic pollutants. J. Environ. Monit. 11, 1117–1304. https://doi.org/10.1039/b823016a.

Chen, Y., Cai, X., Jiang, L., Li, Y., 2016. Prediction of octanol-air partition coefficients for polychlorinated biphenyls (PCBs) using 3D-QSAR models. Ecotoxicol. Environ. Saf. 124, 202–212. https://doi.org/10.1016/j.ecoenv.2015.10.024.

Cheng, H., Deng, Z., Chakraborty, P., Liu, D., Zhang, R., Xu, Y., Luo, C., Zhang, G., Li, J., 2013. A comparison study of atmospheric polycyclic aromatic hydrocarbons in three indian cities using PUF disk passive air samplers. Atmos. Environ. 73, 16–21. https://doi.org/10.1016/j.atmosenv.2013.03.001.

Estellano, V.H., Pozo, K., Harner, T., Franken, M., Zaballa, M., 2008. Altitudinal and seasonal variations of persistent organic pollutants in the Bolivian Andes mountains. Environ. Sci. Technol. 42, 2528–2534. https://doi.org/10.1021/es702754m.

Evci, Y.M., Esen, F., Tasdemir, Y., 2016. Monitoring of long-term outdoor concentrations of PAHs with passive air samplers and comparison with meteorological data. Arch. Environ. Contam. Toxicol. 71, 246–256. https://doi.org/10.1007/s00244-016-0292-6.

Fernández, P., Grimalt, J.O., Vilanova, R.M., 2002. Atmospheric gas-particle partitioning of polycyclic aromatic hydrocarbons in high mountain regions of Europe. Environ. Sci. Technol. 36, 1162–1168. https://doi.org/10.1021/es010190t.

Gouin, T., Harner, T., Blanchard, P., Mackay, D., 2005. Passive and active air samplers as complementary methods for investigating persistent organic pollutants in the Great Lakes Basin. Environ. Sci. Technol. 39, 9115–9122. https://doi.org/10.1021/es051397f.

Gouin, T., Wania, F., Ruepert, C., Castillo, L.E., 2008. Field testing passive air samplers for current use pesticides in a tropical environment. Environ. Sci. Technol. 42, 6625–6630. https://doi.org/10.1021/es8008425.

Grimalt, J.O., Fernandez, P., Berdie, L., Vilanova, R.M., Catalan, J., Psenner, R., Hofer, R., Appleby, P.G., Rosseland, B.O., Lien, L., Massabuau, J.C., Battarbee, R.W., 2001. Selective trapping of organochlorine compounds in mountain lakes of temperate areas. Environ. Sci. Technol. 35, 2690–2697. https://doi.org/10.1021/es000278r.

Guida, Y.de S., Meire, R.O., Torres, J.P.M., Malm, O., 2018. Air contamination by legacy and current-use pesticides in Brazilian mountains: an overview of national regulations by monitoring pollutant presence in pristine areas. Environ. Pollut. 242, 19–30. https://doi.org/10.1016/j.envpol.2018.06.061.

Harner, T., 2021. 2021 v10 Template for Calculating PUF and SIP Disk Sample Air Volumes. https://doi.org/10.13140/RG.2.1.3998.8884.

Harner, T., Bidleman, T.F., 1996. Measurements of octanol-air partition coefficients for polychlorinated biphenyls. J. Chem. Eng. Data 41, 895–899. https://doi.org/10.1021/je960097y.

Harner, T., Su, K., Genualdi, S., Karpowicz, J., Ahrens, L., Mihele, C., Schuster, J., Charland, J.P., Narayan, J., 2013. Calibration and application of PUF disk passive air samplers for tracking polycyclic aromatic compounds (PACs). Atmos. Environ. 75, 123–128. https://doi.org/10.1016/j.atmosenv.2013.04.012.

Hayward, S.J., Gouin, T., Wania, F., 2010. Comparison of four active and passive sampling techniques for pesticides in air. Environ. Sci. Technol. 44, 3410–3416. https://doi.org/10.1021/es902512h.

He, J., Balasubramanian, R., 2010. A comparative evaluation of passive and active samplers for measurements of gaseous semi-volatile organic compounds in the tropical

atmosphere. Atmos. Environ. 44, 884–891. https://doi.org/10.1016/j.atmosenv.2009.12.009.
Heo, J., Lee, G., 2014. Field-measured uptake rates of PCDDs/Fs and dl-PCBs using PUF-disk passive air samplers in Gyeonggi-do, South Korea. Sci. Total Environ. 491–492, 42–50. https://doi.org/10.1016/j.scitotenv.2014.03.073.
Herkert, N.J., Spak, S.N., Smith, A., Schuster, J.K., Harner, T., Martinez, A., Hornbuckle, K.C., 2018. Calibration and evaluation of PUF-PAS sampling rates across the global atmospheric passive sampling (GAPS) network. Environ. Sci. Process. Impacts 20, 210–219. https://doi.org/10.1039/c7em00360a.
Holt, E., Bohlin-Nizzetto, P., Boruvková, J., Harner, T., Kalina, J., Melymuk, L., Klánová, J., 2017. Using long-term air monitoring of semi-volatile organic compounds to evaluate the uncertainty in polyurethane-disk passive sampler-derived air concentrations. Environ. Pollut. 220, 1100–1111. https://doi.org/10.1016/j.envpol.2016.11.030.
Huckins, J.N., Petty, J.D., Lebo, J.A., Almeida, F.V., Booij, K., Alvarez, D.A., Cranor, W.L., Clark, R.C., Mogensen, B.B., 2002. Development of the permeability/performance reference compound approach for in situ calibration of semipermeable membrane devices. Environ. Sci. Technol. 36, 85–91. https://doi.org/10.1021/es010991w.
Jaward, F.M., Zhang, G., Nam, J.J., Sweetman, A.J., Obbard, J.P., Kobara, Y., Jones, K.C., 2005. Passive air sampling of polychlorinated biphenyls, organochlorine compounds, and polybrominated diphenyl ethers across Asia. Environ. Sci. Technol. 39, 8638–8645. https://doi.org/10.1021/es051382h.
Kalina, J., Scheringer, M., Boruvková, J., Kukucka, P., Pribylová, P., Bohlin-Nizzetto, P., Klánová, J., 2017. Passive air samplers as a tool for assessing long-term trends in atmospheric concentrations of semivolatile organic compounds. Environ. Sci. Technol. 51, 7047–7054. https://doi.org/10.1021/acs.est.7b02319.
Kennedy, K., Hawker, D.W., Bartkow, M.E., Carter, S., Ishikawa, Y., Mueller, J.F., 2010. The potential effect of differential ambient and deployment chamber temperatures on PRC derived sampling rates with polyurethane foam (PUF) passive air samplers. Environ. Pollut. 158, 142–147. https://doi.org/10.1016/j.envpol.2009.07.031.
Klánová, J., Èupr, P., Kohoutek, J., Harner, T., 2008. Assessing the influence of meteorological parameters on the performance of polyurethane foam-based passive air samplers. Environ. Sci. Technol. 42, 550–555. https://doi.org/10.1021/es072098o.
Li, Y., Geng, D., Liu, F., Wang, T., Wang, P., Zhang, Q., Jiang, G., 2012. Study of PCBs and PBDEs in King George Island, Antarctica, using PUF passive air sampling. Atmos. Environ. 51, 140–145. https://doi.org/10.1016/j.atmosenv.2012.01.034.
Mari, M., Schuhmacher, M., Feliubadaló, J., Domingo, J.L., 2008. Air concentrations of PCDD/Fs, PCBs and PCNs using active and passive air samplers. Chemosphere 70, 1637–1643. https://doi.org/10.1016/j.chemosphere.2007.07.076.
Marklund, A., Andersson, B., Haglund, P., 2005. Traffic as a source of organophosphorus flame retardants and plasticizers in snow. Environ. Sci. Technol. 39, 3555–3562. https://doi.org/10.1021/es0482177.
Markovic, M.Z., Prokop, S., Staebler, R.M., Liggio, J., Harner, T., 2015. Evaluation of the particle infiltration efficiency of three passive samplers and the PS-1 active air sampler. Atmos. Environ. 112, 289–293. https://doi.org/10.1016/j.atmosenv.2015.04.051.
Meire, R.O., Lee, S.C., Targino, A.C., Torres, J.P.M., Harner, T., 2012. Air concentrations and transport of persistent organic pollutants (POPs) in mountains of southeast and southern Brazil. Atmos. Pollut. Res. 3, 417–425. https://doi.org/10.5094/APR.2012.048.
Moeckel, C., Harner, T., Nizzetto, L., Strandberg, B., Lindroth, A., Jones, K.C., 2009. Use of depuration compounds in passive air samplers: results from active sampling-supported field deployment, potential uses, and recommendations. Environ. Sci. Technol. 43, 3227–3232. https://doi.org/10.1021/es802897x.
Odabasi, M., Cetin, E., Sofuoglu, A., 2006. Determination of octanol-air partition coefficients and supercooled liquid vapor pressures of PAHs as a function of temperature: application to gas-particle partitioning in an urban atmosphere. Atmos. Environ. 40, 6615–6625. https://doi.org/10.1016/j.atmosenv.2006.05.051.
Okeme, J.O., Rodgers, T.F.M., Jantunen, L.M., Diamond, M.L., 2018. Examining the gas-particle partitioning of organophosphate esters: how reliable are air measurements? Environ. Sci. Technol. 52, 13834–13844. https://doi.org/10.1021/acs.est.8b04588.
Pozo, K., Harner, T., Wania, F., Muir, D.C.G.G., Jones, K.C., Barrie, L.A., 2006. Toward a global network for persistent organic pollutants in air: results from the GAPS study. Environ. Sci. Technol. 40, 4867–4873. https://doi.org/10.1021/es060447t.
Pozo, K., Harner, T., Lee, S.C., Wania, F., Muir, D.C.G., Jones, K.C., 2009. Seasonally resolved concentrations of persistent organic pollutants in the global atmosphere from the first year of the GAPS study. Environ. Sci. Technol. 43, 796–803. https://doi.org/10.1021/es802106a.
Pozo, K., Estellano, V.H., Harner, T., Diaz-Robles, L., Cereceda-Balic, F., Etcharren, P., Pozo, Katerine, Vidal, V., Guerrero, F., Vergara-Fernández, A., 2015. Assessing polycyclic aromatic hydrocarbons (PAHs) using passive air sampling in the atmosphere of one of the most wood-smoke-polluted cities in Chile: the case study of Temuco. Chemosphere 134, 475–481. https://doi.org/10.1016/J.CHEMOSPHERE.2015.04.077.
Pozo, K., Martellini, T., Corsolini, S., Harner, T., Estellano, V., Kukucka, P., Mulder, M.D., Lammel, G., Cincinelli, A., 2017. Persistent organic pollutants (POPs) in the atmosphere of coastal areas of the Ross Sea, Antarctica: indications for long-term downward trends. Chemosphere 178, 458–465. https://doi.org/10.1016/j.chemosphere.2017.02.118.
Prats, R.M., van Drooge, B.L., Fernández, P., Marco, E., Grimalt, J.O., 2021. Changes in urban gas-phase persistent organic pollutants during the COVID-19 lockdown in Barcelona. Front. Environ. Sci. 9, 109. https://doi.org/10.3389/fenvs.2021.650539.
Rauert, C., Harner, T., Schuster, J.K., Quinto, K., Fillmann, G., Castillo, L.E., Fentanes, O., Ibarra, M.V., Miglioranza, K.S.B., Rivadeneira, I.M., Pozo, K., Puerta, A.P., Zuluaga, B.H.A., 2016. Towards a regional passive air sampling network and strategy for new POPs in the GRULAC region: perspectives from the GAPS network and first results for organophosphorus flame retardants. Sci. Total Environ. 573, 1294–1302. https://doi.org/10.1016/j.scitotenv.2016.06.229.
Ren, J., Wang, X., Xue, Y., Gong, P., Joswiak, D.R., Xu, B., Yao, T., 2014. Persistent organic pollutants in mountain air of the southeastern Tibetan Plateau: seasonal variations and implications for regional cycling. Environ. Pollut. 194, 210–216. https://doi.org/10.1016/j.envpol.2014.08.002.
Saini, A., Clarke, J., Harner, T., 2019. Direct measurements of polyurethane foam (PUF) – air partitioning coefficients for chemicals of emerging concern capable of equilibrating in PUF disk samplers. Chemosphere 234, 925–930. https://doi.org/10.1016/j.chemosphere.2019.06.134.
Salamova, A., Ma, Y., Venier, M., Hites, R.A., 2013. High levels of organophosphate flame retardants in the Great Lakes atmosphere. Environ. Sci. Technol. Lett. 1, 8–14. https://doi.org/10.1021/ez400034n.
Shoeib, M., Harner, T., 2002. Characterization and comparison of three passive air samplers for persistent organic pollutants. Environ. Sci. Technol. 36, 4142–4151. https://doi.org/10.1021/es020635t.
Stein, A.F., Draxler, R.R., Rolph, G.D., Stunder, B.J.B., Cohen, M.D., Ngan, F., 2015. Noaa's hysplit atmospheric transport and dispersion modeling system. Bull. Am. Meteorol. Soc. 96, 2059–2077. https://doi.org/10.1175/BAMS-D-14-00110.1.
Sühring, R., Wolschke, H., Diamond, M.L., Jantunen, L.M., Scheringer, M., 2016. Distribution of organophosphate esters between the gas and particle phase-model predictions vs measured data. Environ. Sci. Technol. 50, 6644–6651. https://doi.org/10.1021/acs.est.6b00199.
Tuduri, L., Harner, T., Hung, H., 2006. Polyurethane foam (PUF) disks passive air samplers: wind effect on sampling rates. Environ. Pollut. 144, 377–383. https://doi.org/10.1016/j.envpol.2005.12.047.
Van der Veen, I., de Boer, J., 2012. Phosphorus flame retardants: properties, production, environmental occurrence, toxicity and analysis. Chemosphere 88, 1119–1153. https://doi.org/10.1016/j.chemosphere.2012.03.067.
Van Drooge, B.L., Ballesta, P.P., 2009. Seasonal and daily source apportionment of polycyclic aromatic hydrocarbon concentrations in PM10 in a semirural european area. Environ. Sci. Technol. 43, 7310–7316. https://doi.org/10.1021/es901381a.
Van Drooge, B.L., Grimalt, J.O., 2015. Particle size-resolved source apportionment of primary and secondary organic tracer compounds at urban and rural locations in Spain. Atmos. Chem. Phys. 15, 7735–7752. https://doi.org/10.5194/acp-15-7735-2015.
Van Drooge, B.L., Grimalt, J.O., Torres García, C.J., Cuevas, E., 2002. Semivolatile organochlorine compounds in the free troposphere of the Northeastern Atlantic. Environ. Sci. Technol. 36, 1155–1161. https://doi.org/10.1021/es010189u.
Van Drooge, B.L., Grimalt, J.O., Camarero, L., Catalan, J., Stuchlík, E., Torres García, C.J., 2004. Atmospheric semivolatile organochlorine compounds in European high-mountain areas (Central Pyrenees and High Tatras). Environ. Sci. Technol. 38, 3525–3532. https://doi.org/10.1021/es030108p.
Van Drooge, B.L., Grimalt, J.O., Booij, K., Camarero, L., Catalan, J., 2005. Passive sampling of atmospheric organochlorine compounds by SPMDs in a remote high mountain area. Atmos. Environ. 39, 5195–5204. https://doi.org/10.1016/j.atmosenv.2005.05.020.
Van Drooge, B.L., Fernández, P., Grimalt, J.O., Stuchlík, E., García, C.J.T., Cuevas, E., 2010. Atmospheric polycyclic aromatic hydrocarbons in remote european and Atlantic sites located above the boundary mixing layer. Environ. Sci. Pollut. Res. 17, 1207–1216. https://doi.org/10.1007/s11356-010-0296-0.
Wang, Q., Zhao, H., Wang, Y., Xie, Q., Chen, J., Quan, X., 2017. Determination and prediction of octanol-air partition coefficients for organophosphate flame retardants. Ecotoxicol. Environ. Saf. 145, 283–288. https://doi.org/10.1016/j.ecoenv.2017.07.040.
Wania, F., MacKay, D., 1996. Tracking the distribution of persistent organic pollutants. Environ. Sci. Technol. 30, 390A–396A. https://doi.org/10.1021/es962399q.
Wania, F., Shunthirasingham, C., 2020. Passive air sampling for semi-volatile organic chemicals. Environ. Sci. Process. Impacts 22, 1919–2134. https://doi.org/10.1039/d0em00194e.
Yeo, H.G., Choi, M., Chun, M.Y., Sunwoo, Y., 2003. Gas/particle concentrations and partitioning of PCBs in the atmosphere of Korea. Atmos. Environ. 37, 3561–3570. https://doi.org/10.1016/S1352-2310(03)00361-3.
Zhang, G., Chakraborty, P., Li, J., Sampathkumar, P., Balasubramanian, T., Kathiresan, K., Takahashi, S., Subramanian, A., Tanabe, S., Jones, K.C., 2008. Passive atmospheric sampling of organochlorine pesticides, polychlorinated biphenyls, and polybrominated diphenyl ethers in urban, rural, and wetland sites along the coastal length of India. Environ. Sci. Technol. 42, 8218–8223. https://doi.org/10.1021/es8016667.
Zhang, X., Hoang, M., Lei, Y.D., Wania, F., 2015. Exploring the role of the sampler housing in limiting uptake of semivolatile organic compounds in passive air samplers. Environ. Sci. Process. Impacts 17, 1995–2136. https://doi.org/10.1039/c5em00447k.
Zhu, N., Schramm, K.W., Wang, T., Henkelmann, B., Zheng, X., Fu, J., Gao, Y., Wang, Y., Jiang, G., 2014. Environmental fate and behavior of persistent organic pollutants in Shergyla Mountain, southeast of the Tibetan Plateau of China. Environ. Pollut. 191, 166–174. https://doi.org/10.1016/j.envpol.2014.04.031.